In Situ Ultrasonic Monitoring of Aluminum Ion Hydrolysis in Aqueous Solutions: Instrumentation, Techniques, and Comparisons to pH-Metry

Alexander N. Kalashnikov, *Member, IEEE*, Kirill L. Shafran, Vladimir G. Ivchenko, Richard E. Challis, and Carole C. Perry

***Abstract*—A cross-disciplinary experimental study related to both ultrasonic instrumentation and analytical chemistry is reported. The hydrolysis process was conducted by time-resolved titration in a fully automated manner. Acquired ultrasonic records were processed in order to estimate the propagation delay of the ultrasonic pulse in the evolving medium. The limited hardware resolution of two different ultrasonic instruments employed was improved by calculating the center of gravity of the recorded pulses. Application of signal averaging to the acquisition of raw records in the custom-built instrument eliminated spurious records almost completely. The estimated ultrasonic delays were corrected for temperature changes that were measured independently. This procedure transformed the ultrasonic titration curves into two almost straight lines that intersected at the equivalence point. The results obtained showed that it was possible to detect changes as small as 200 ppm by using the ultrasonic instrument *in situ* at significantly lower setting times compared to a conventional pH-meter.**

***Index Terms*—Aluminum hydroxide, group delay estimation, monitoring of hydrolysis, pH and ultrasonic titration curves, signal averaging, time resolved acid-base titration, ultrasonic measurements.**

I. Introduction

COMPLEX chemical processes in aqueous solutions can be resolved by using various analytical instruments, with optical spectroscopy methods being the "most widely used tools for the elucidation of the structure of molecular species, as well as the quantitative and qualitative determination of both organic and inorganic compounds" [1]. However, these methods can be difficult to apply *in situ*, online, and for opaque media. Some other conventional analytical methods (e.g., electroanalytical techniques) can only provide single point values for a sample solution or they may introduce tough requirements for the sample homogeneity/mixing efficiency. These limitations can be avoided by using ultrasound that can propagate in opaque media and can acquire information related to its propagation along the entire pathway. This feature provides a potential for imaging the entire reaction vessel ultrasonically.

Propagation of ultrasound in aqueous solution can be considered from the prospective of phase velocity, attenuation (optionally, versus frequency), and group velocity. As the wavelength of ultrasound in water is on the order of at least tens of micrometers or more for frequencies up to 150 MHz, resonant absorption does not take place normally, and attenuation versus frequency represents smooth curves [2]. The intensity of ultrasound applied to a monitored medium should be small to avoid heating and other alterations to the medium (although ultrasound is used in analytical chemistry for invasive sample preparation as well [3]), and undesirable effects on another analytical instruments [4].

Propagation of ultrasound in electrolytes was studied extensively "based on the ionic-atmosphere model developed by Debye and Hückel in 1923" [5, p. 354] with further refinements. It qualitatively or partially quantitatively described some experimental phenomena related to the dependence of ultrasound velocity on the concentration of electrolyte. This theory was not extended toward nonelectrolytes, and its experimental verification was complicated seriously by the low resolution of the previous generation of instruments and strong dependence of ultrasound on temperature that complicated accurate measurements [5].

Various theories based on consideration of relaxation phenomena (thermal [6], [7], structural [6], [8], chemical [6], and shear [8]) led to development of ultrasonic models that qualitatively and quantitatively described ultrasonic absorption in homogeneous media versus frequency at different temperatures. This approach has been extended further for binary mixtures like colloids, emulsions, etc. [2].

Some phenomenological macroscopic models for determining ultrasonic velocities in binary and ternary mixtures were applied to experimental data in [9], but only a partial fit was achieved.

Overall, although theoretical models for both ultrasonic velocity and attenuation have been elaborated and extensively refined for stationary conditions in a chemical sense, they could be difficult to apply for evolving media.

Another approach to ultrasonic monitoring is based on experimental rather than theoretical considerations. Ultrasound velocity and attenuation were found sensitive to a range of physical–chemical transformations (e.g., [2], [10], and [11]).

Manuscript received June 30, 2006; revised April 20, 2007. This work was supported by the U.K. Engineering and Physical Sciences Research Council. This paper has been based on a presentation made at IMTC-06 (IM-6277 [18]).

A. N. Kalashnikov, V. G. Ivchenko, and R. E. Challis are with the School of Electrical and Electronic Engineering, University of Nottingham, NG7 2RD Nottingham, U.K. (e-mail: alexander.kalashnikov@nottingham.ac.uk; vladimir.ivchenko@nottingham.ac.uk; richard.challis@nottingham.ac.uk).

K. L. Shafran and C. C. Perry are with the School of Biomedical and Natural Sciences, Nottingham Trent University, NG1 4BU Nottingham, U.K. (e-mail: kirill.shafran@ntu.ac.uk; carole.perry@ntu.ac.uk).

Digital Object Identifier 10.1109/TIM.2007.899857

These experimental observations encouraged further phenomenological and empirical studies.

In this paper, we discuss our observations on different methods of analysis of ultrasound signals propagating through a chemically evolving aqueous solution and compare the ultrasonic titration curve with the conventional pH one.

II. Description of the Chemical Process Observed

This paper involves the titration of an aqueous solution containing Al^{3+} ions (sample) by the addition of hydroxide ions OH^- (titrant) in a similar fashion to our previous studies [12], [13]. Simplified description of this process can be narrowed down to two main stages. Before the equivalence point at pH $\sim$7, the precipitate of aluminum hydroxide is gradually formed:

$$Al^{3+}(aq) + OH^-(aq) \rightarrow Al(OH)_3(s). \quad (1)$$

The solubility product constant for this reaction is 2×10^{-31} [14, p. 463] that indicates a one-way process. After the equivalence point, the formation of aluminate-ions $Al(OH)_4^-$ occurs

$$Al(OH)_3(s) + OH^-(aq) \rightarrow Al(OH)_4^-(aq). \quad (2)$$

The constant for this formation is 10^{33} [14, p. 453] and thus, a one-way process occurs here as well.

A more rigorous description of the complex chemical processes involved can be found elsewhere (e.g., [12] and [13]). The first overall reaction eventually leads to the formation of amorphous Al hydroxide, which is quite common in nature (it can be found in soils, sediments, and in a number of minerals) and it has numerous industrial applications in ceramics, such as chromatographic phase, catalyst carrier, adjuvant, antacid, flocculant for water purification, etc. [15]. There have been indications in the literature that Al hydroxide can be an important source of toxic ionic forms of aluminum upon acidification of environmental waters [16, pp. 110 and 455].

III. Automated Experimental Setup and Description of the Experiments Conducted

One of particular objectives of this paper was to test feasibility of ultrasonic monitoring in an environment similar to a conventional chemical laboratory or a production plant. The experiments, when started, remained fully autonomous until the process completed. This was accomplished by use of automatic liquid handling unit that operated in a time-resolved titration mode, and various instruments that continuously recorded different process parameters using a personal computer [17, Fig. 1, Tab. I].

The list of the experiments conducted is presented in Table II. It includes description of samples, titrants used, and Brønsted–Lowry classification in the first two columns. The third column presents number of titrant additions, the interval between them, and the change of chemical composition after the first titrant addition in weight ppm. The next column describes when the equivalence point occurred in terms of titrant volumes and time on the time-resolved titration curves

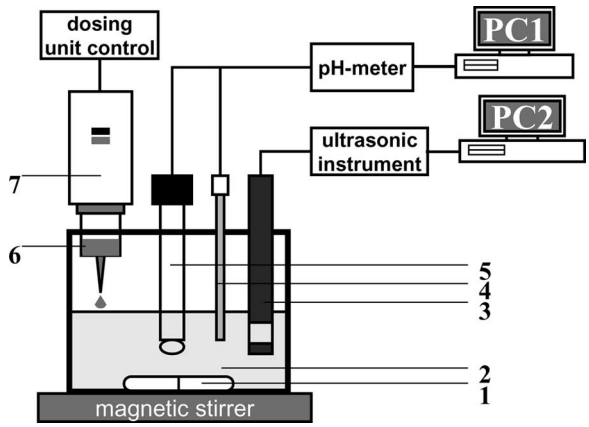

Fig. 1. Schematic of the experimental setup (1—magnetic stirrer, 2—aqueous solution, 3—ultrasonic probe consisted of a transducer and a reflector, 4—temperature probe, 5—pH electrode, 6—removable tip, 7—liquid handling unit).

where applicable. The subsequent column indicates the change of temperature during the course of the experiments. The following column presents a nominal delay of ultrasound pulse propagation from the ultrasonic transducer to the reflector and back τ_0 (pulse-echo mode was used). In the following two columns, the observed changes of the ultrasonic delay are presented. It was found that this delay slowly increased up to the equivalent point and then steadily decreased, where observed. For experiments 1 and 5, this delay decreased continuously. These columns show that the magnitude of change observed was very small compared to τ_0 and could vary in an order of magnitude for different titrants. The "instruments used" column completes Table II.

IV. Selection of an Appropriate Metric for Ultrasonic Monitoring

A raw ultrasonic record presents a modulated pulse that changes very little between records visually [18, Fig. 2]. The ensemble of acquired records can be processed in a number of ways, both in the time and frequency (via the Fourier transform) domains, giving several possible metrics suitable for use in monitoring. It seems desirable to select only a few if not a single parameter that is not only sensitive to chemical changes, but is resilient to noise as well. A single parameter is easier to track, check, and control in a laboratory, a pilot plant, or in a field [19]. The importance of the noise resilience is dictated by propagation losses in the electroacoustic pathway. The losses could start from about 40 dB, even for a lightly absorbing medium like water, and increase along with the operating frequency and the gauge length heavily (at least exponentially). Therefore, ultrasonic instruments operate at low signal-to-noise ratio (SNR), and the noise influence could significantly affect the measurement uncertainty particularly if a nonlinear processing is employed [20].

The clarity of ultrasonic records depends on the sampling frequency, number of bits of an analog-to-digital converter (ADC) used, and the input SNR. Two different instruments were used in the experiments reported here (Table I), and the constant ratio of the sampling frequency to the central

TABLE I
INSTRUMENTS USED

No	Model of the instrument	Instrument's maker	Purpose of the instrument	Relevant parameters/features
1	V309-SU	Panametrics	Ultrasonic transducer	Central frequency 5 MHz, used with instruments 4,5
2	V317-SU	Panametrics	"-"	Central frequency 20 MHz, used with instrument 3
3	Arbitrary function generator (AFG)	NDT Solutions	Complete ultrasonic instrument	Sampling frequency 320 MHz ADC resolution 8 bits Interval between records 2 s Number of averages 1
4	N/A	Custom built in the University of Nottingham	Back end of an ultrasonic instrument	Sampling frequency 80 MHz ADC resolution 14 bits Interval between records 0.5 s Number of averages 1024
5	Ultrasonic pulser receiver (UPR)	NDT Solutions	Front end of an ultrasonic instrument	Adjustable duration of an excitation rectangular pulse Adjustable gain for received pulses
6	PHM 240 with Red Rod glass electrode	Radiometer	PH meter	Resolution 0.002 units pH Resolution 0.1°C
7	EDOS 5222	Eppendorf	Automatic liquid handling unit	Periodical automatic dispensing of preset volumes of liquids

Conventional laboratory stand, glassware, magnetic stirrer

TABLE II
EXPERIMENTS CONDUCTED

No	Sample	Titrant, its concentration (M) and volume of a single drop	Number of drops, time interval in between, change in ppm	Equivalence point	t_{min}/ t_{max}	τ_0 μs	$\Delta\tau$ (rise) ns	$\Delta\tau$ (fall) ns	Instruments used
1	HCl (SA*) 0.169 M 100 mL	$AlCl_3$ (WA*) 0.635 M 0.4 mL	60 30 s 300 ppm	N/A	24°C 24.1°C	6	--	50	1,3,6,8
2	$AlCl_3$ (WA*) 0.1156 M 100 mL	KOH (SB*) 2.863 M 0.2 mL	80 60 s 210 ppm	60 drops	24.6°C 26.9°C	13	40	54	1,3,6,8
3	$AlCl_3$ (WA*) 0.0625 M 160 mL	NaOH (SB*) 1.0060 M 0.8 mL	50 30 s 210 ppm	37.2 drops 38*30+60= 1200 s	19.4°C 20.8°C	7	3.8	21	2,4-9
4	$AlCl_3$ (WA*) 0.0666 M 150 mL	NH_4OH (WB*) 0.8 M 1 mL	50 30 s 200 ppm	37.5 drops 38*30+60= 1200 s	17.8°C 19.4°C	7	17.5	3.8	2, 4-9
5	$AlCl_3$ (WA*) 0.0666 M 150 mL	Na_2SO_4 (WA*) 0.4 M 1 mL	50 30 s 440 ppm	N/A	19.6°C 20.8°C	7	---	59	2, 4-9

*W/S – weak/strong; A/B – acid/base

frequency of the transducer of 16 was used. For the of-the-shelf instrument (arbitrary function generator [21]), some spurious records were to be eliminated from the consideration. This elimination was based on the correlation analysis that rejected records dissimilar to their neighbor [18, Sec. 4.1]. Although this instrument was capable of averaging, it took tens of seconds to complete due to its software implementation that was too slow to be used. The second (custom built by the authors) instrument featured "on-the-fly" averaging architecture [22], and averaging of 1024 records was completed in less than a second. The aforementioned preselection procedure was found redundant for the averaged records.

Several parameters were extracted from the experimental records, such as maximal absolute value, standard deviation, maximal value among spectral components and the corresponding frequency, and amplitude at the central frequency of the

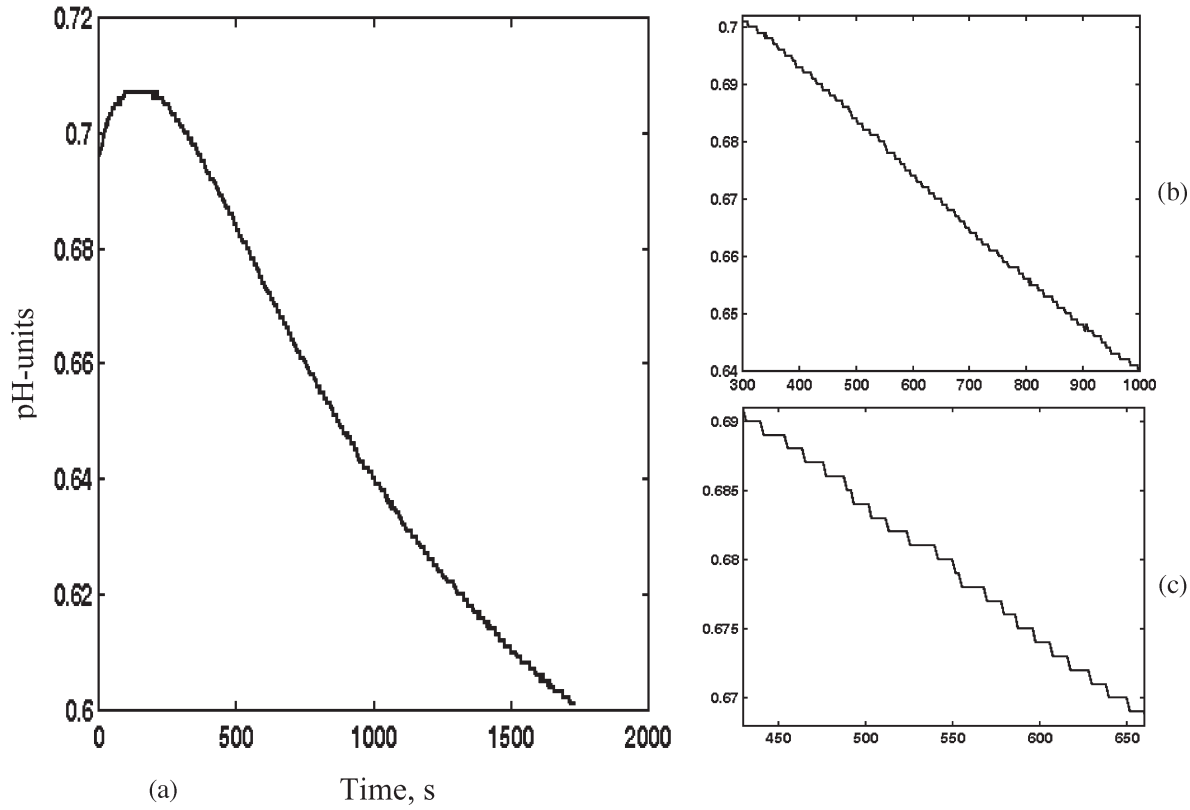

Fig. 2. pH titration curve for experiment 1. (Left) Overall. (Right) Zoomed fragments.

transducer [18, Sec. 4.3-4]. The time domain position of the pulse peak was found most promising, but the native hardware resolution in the time domain was found to be insufficient for the comprehensive analysis. A better alternative was to consider the center of gravity (CoG) of the recorded pulse that was estimated as

$$\mathrm{CoG} = \frac{\int t s^2(t) dt}{\int s^2(t) dt} = \frac{\sum n s_n^2}{\sum s_n^2} \tag{3}$$

where $s(t)$ is the continuous signal of interest, and s_n are its samples. This parameter is very similar to the "midpoint of the received envelope" [23] and to the "center of area" [24] parameters that were used for estimation of delay times by other authors. An important advantage of using the CoG and similar measures is their insensitivity to changes in amplitude of the recorded signal that occur, for example, due to spontaneous bubble formation on the surface of the transducer and/or the reflector.

For the above reasons, the delay of the ultrasonic signal was selected as a monitored parameter, and it was estimated on the basis of the CoG that allowed the improvement of the hardware resolution at about one order of magnitude.

V. Comparison of Ultrasonic Delay and pH Titration Curves for Experiments 1, 2

In experiment 1, a $AlCl_3$ (0.4 M) solution was added to an HCl (0.943 M) solution (Table I). The Al chloride concentration was increased by introducing strongly acidic conditions to prevent possible autohydrolysis. After the first additions of Al salt, the pH value was increasing (Fig. 2), due to conversion of $Al(OH)_2^+$ and other possible hydrolyzed species back to aluminum hexaaquocation $[Al(H_2O)_6]^{3+}$ at very low pH of HCl solution, as follows:

$$[\mathrm{Al(OH)}_x(\mathrm{H_2O})_{6-x}]^{(3-x)} + x\mathrm{H}^+ \rightleftharpoons [\mathrm{Al(H_2O)_6}]^{3+}. \tag{4}$$

When all hydrolyzed Al species were converted into hexaaquocation $Al(H_2O)_6$, the value of pH started decreasing steadily and nonlinearly (Fig. 2). The pH titration curve for the experiment 1 [Fig. 2(a)] shows a smooth profile that is linear piecewise [Fig. 2(b)]. A closer view [Fig. 2(c)] reveals the actual stepwise shape of the pH curve. In contrast, the ultrasonic delay curve is practically linear throughout the titration [Fig. 3(a)]. The steps on the curve after each titrant addition are also present, although slightly scattered at closer inspection [Fig. 3(b)]. The ultrasonic delay data presented as CoGs [Fig. 3(c)] shows improved stepwise shape of the curve, which potentially would allow for monitoring of chemical compositions in the HCl–$AlCl_3$ aqueous mixture.

Experiment 2 (see Table II for experimental details) represents the titration of 0.4-M $AlCl_3$ aqueous solution with strong alkali (KOH). The pH-metric titration curve is presented in Fig. 4(a). A substantial stabilization time up to 20 s was observed for this curve [Fig. 4(b)–(d)]. The transitions between each titrant drop were caused by 1) a relatively slow hydrolysis-condensation processes with time scales significantly longer

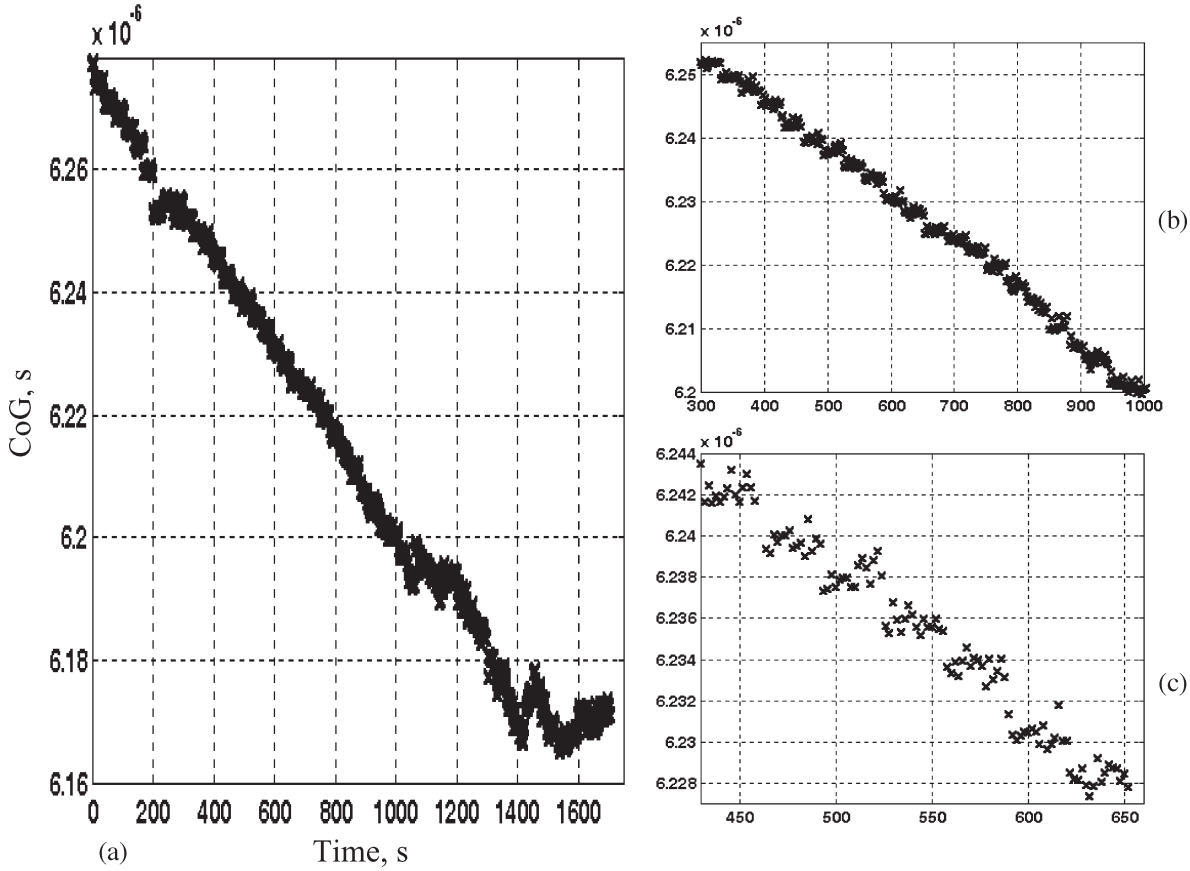

Fig. 3. Ultrasonic titration curve for the experiment 1. (Left) Overall. (Right) Zoomed fragments.

than the time gap between titrant additions (varied between 30 and 120 s); 2) relatively slow response times of an otherwise very fast RedRod combined glassy pH-electrode at certain unfavorable conditions for pH measurements, including formation of the viscous sol of Al hydroxide particles beginning to appear at hydrolysis ratio $h > 2.0$ (the ratio between the concentration of Al^{3+} ions to the concentration of the OH^- ions, it was proportional to the experiment time); and (c) imperfect mixing occurring due to increasing viscosity of the condensing Al-ion medium at reasonably high hydrolysis ratios.

The CoG data calculated from ultrasonic delay measurements shows much quicker equilibration behavior and practically flat steps on the titration curve [Fig. 5(b)]. The time of stabilization of ultrasonic delay around some average value after each addition of titrant does not exceed ~5 s during the course of experiment 2. Since ultrasonic parameters are free of the stabilization problems related to pH-metry discussed above, this value of ~5 s is a good estimate of the maximum time required for complete mixing of a new titrant portion with the bulk sample.

The shape of the ultrasonic delay curve as a function of experiment time [Fig. 5(a)] appears to show an apparently reverse trend to that of the pH-metric curve up to titration time of 3000 s. At this point, corresponding to hydrolysis ratio $h = 3.0$ and the major inflexion on pH-metric curve, ultrasonic delay indicates a local maximum followed by a sharp decrease of ultrasonic delay above ca. 3200–3400 s. From a chemical point of view, this behavior of ultrasonic delay looks irregular, as increasingly condensed Al species, including small Al oligomers (dimers, trimers) and large amounts of Al_{13}-mer dominating in mildly acidic conditions (up to pH ~4.6) decrease the effective degree of freedom of the system. That is because most Al ions are bonded to each other by hydroxo(oxo)-bridges. It could be expected that, with dynamic viscosity and density of the hydrolyzed Al-ion solution remaining nearly constant at pH ~4.6, condensation into Al polycations would ideally result in slow but steady increase of ultrasonic delay. Instead, the experimental data shows an opposite trend. Ionic strength of the solution should remain mainly unchanged at the titration stages preceding the formation of Al hydroxide colloids. The stability of ionic strength is achieved by compensation of increasing concentration of added alkali (particularly K^+ ion) by constant elimination of OH^--ions in the condensation reactions of Al-ions below the hydrolysis ratio $h = 3.0$.

At hydrolysis ratios higher than 3.0, an increase of the total ionic strength takes place. This is because hydroxide ions are no longer consumed by condensation reactions above electroneutrality point of Al hydroxide (pH ~7; $h = 3.0$). These ions contribute to 1) rapidly increasing pH of the titrated sample and 2) rapidly increasing total ionic strength. This explains well the rapidly decreasing part of the delay-based titration curve above the point of neutralization [Fig. 5(a), $t > 3400$ s].

It could be assumed that in the absence of significant contributions from such factors as solution density, viscosity, solute

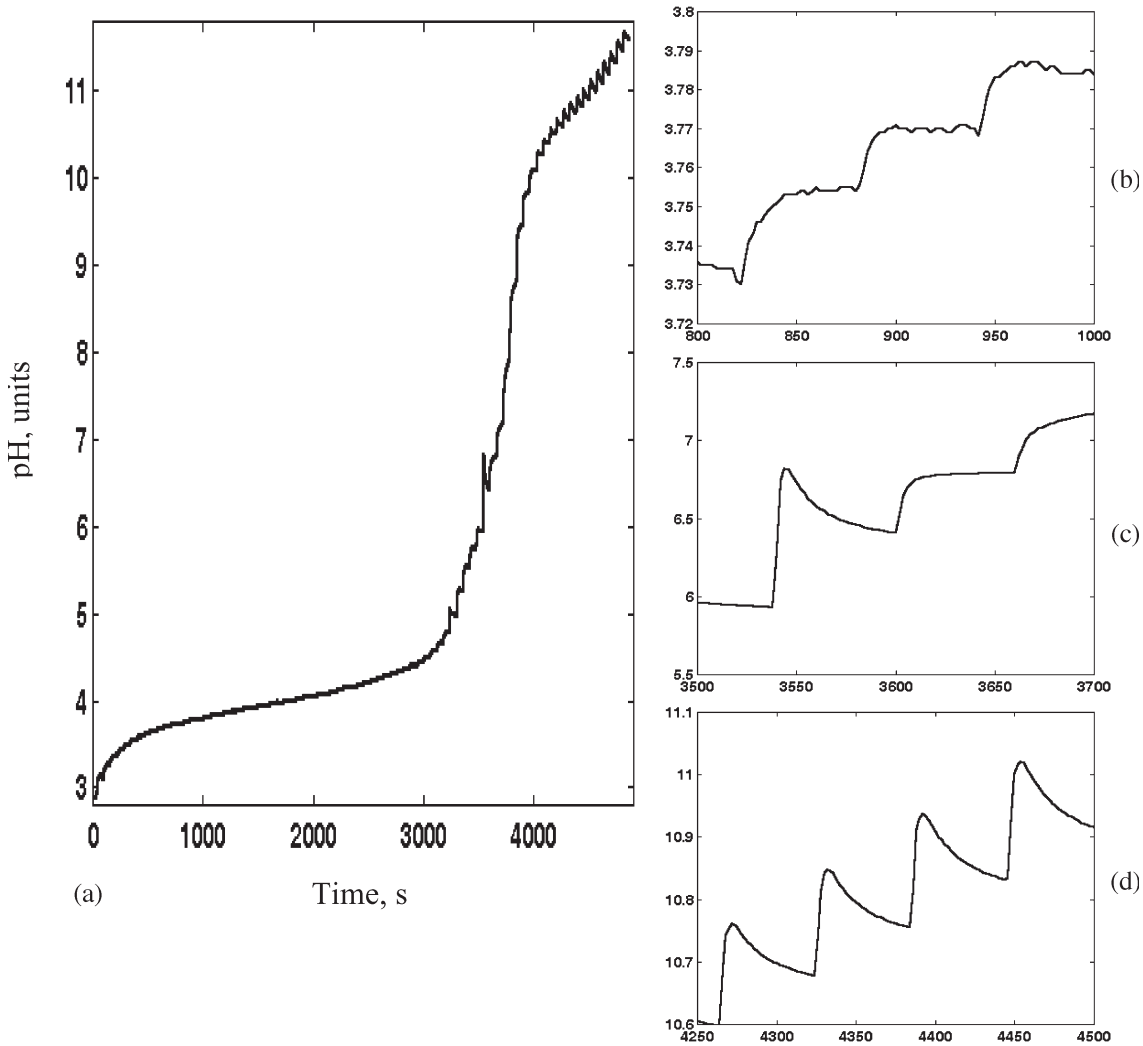

Fig. 4. pH titration curve for the experiment 2. (Left) Overall. (Right) Zoomed fragments.

concentration, the apparently reverse trend of ultrasonic delay data in comparison with pH-metric data at $h < 2.0$ ($t < 3000$ s) is a consequence of large temperature variations during the titration, which has been found to be within $\sim$2.3 °C for the experiment 2. It is well known that hydrolysis and condensation of Al-ions are exothermic reactions releasing significant amounts of heat throughout the process of neutralization with base [14]. The largest exothermic effect is usually observed at the early stages of Al-ion hydrolysis ($h < 1.0$), and the heat release stops after the hydrolysis ratio of 3.0 is reached, i.e., above the point of bulk precipitation of Al hydroxide. The described increase of the temperature of solution due to exothermic hydrolytic reactions of Al-ions could explain well the decrease of ultrasonic delay at $h < 2.0$ ($t < 3000$ s) observed in the experiment 2 and other acid-base titration experiments in this paper.

VI. Computational Compensation of the Temperature Effect on the Ultrasonic Records

As the velocity of ultrasound depends on temperature in water strongly [25], ultrasonic measurements are carried out in thermocontrolled chambers frequently. Our experiments were carried out in an open laboratory space. Therefore, some temperature changes were observed and recorded using a conventional temperature sensor built into the pH-meter of resolution 0.1 °C. In experiment 2, the temperature rose 2.3 °C up to the equivalence point [Fig. 6(a)] because of the exothermic effect of the neutralization reaction. To compensate for that, the CoGs determined from the experimental records were corrected using the following expression [26]:

$$\mathrm{CoG_{corr}} = \mathrm{CoG} + \mathrm{mean(CoG)} \times 2.5 \times [\mathrm{mean}(T) - T]\,/1500 \tag{5}$$

where T is the temperature, and constants 2.5 and 1500 represent the actual gradient and the absolute value of the ultrasound velocity, respectively. These constants are close to those for water, and their use seems appropriate because of low molarity of the solutions used. The effect of these corrections is shown in Fig. 6(b), where the experimental CoGs were assumed to be constant and equal to the CoG at the start of the experiment 2. The concavity of the simulated ultrasonic delay is opposite to

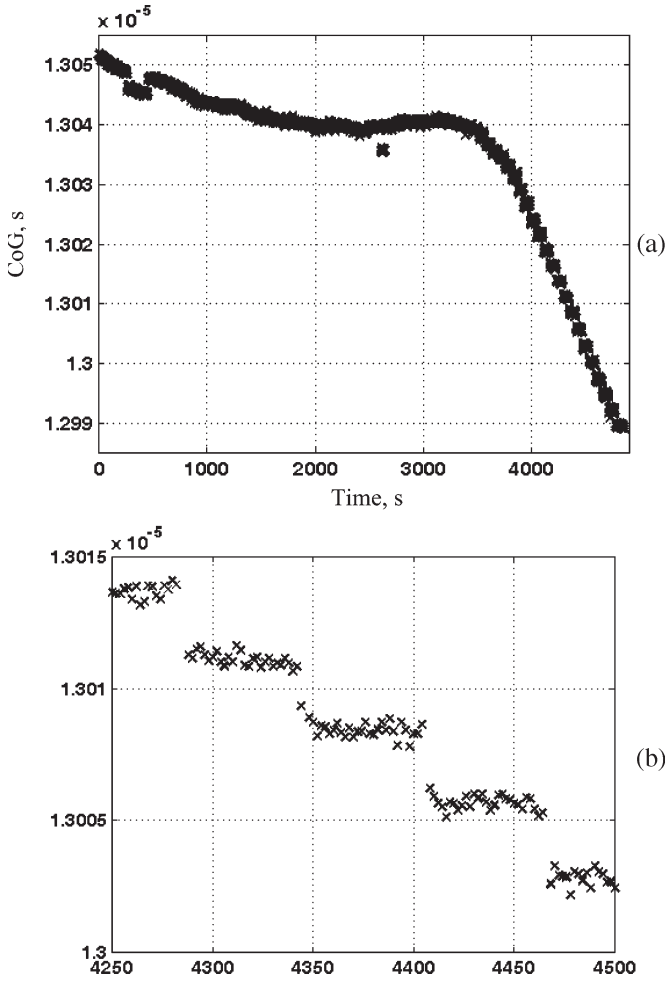

Fig. 5. Ultrasonic titration curve for the experiment 2. (Top) Overall. (Bottom) Zoomed fragment.

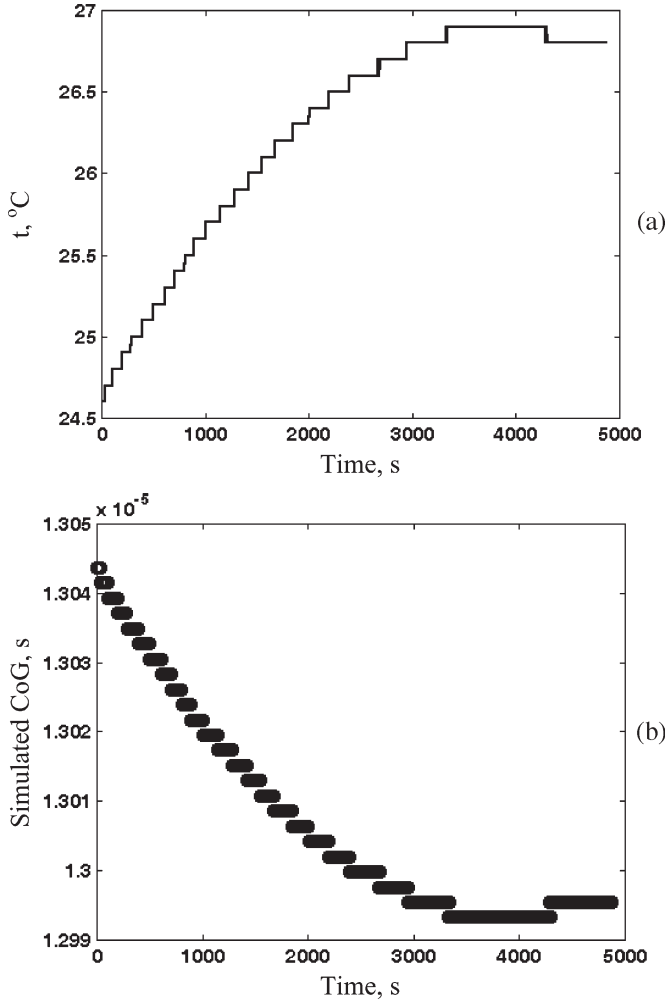

Fig. 6. (a) Recorded temperatures and (b) derived propagation times for experiment 2.

the experimental one, and the amount of change is about the same as observed in the experiment. That is why the application of the correction (6) transformed the experimental CoG curve quite substantially as shown in Fig. 7(a). (Temperature readings were transformed from discrete experimental points [Fig. 7(b), dashed line] into a continuous curve [Fig. 7(b), solid line] using spline interpolation.) The magnified part of the corrected titration curve shows a clear maximum approximately corresponding to complete neutralization of Al hydroxide at $h = 3.0$ (Fig. 8), and almost straight line changes beyond it. The decreasing part of the temperature curve in Fig. 8 shows that approximately four titrant additions were required to change the CoG on $\sim$5 ns. This time corresponds to about 1.25-ns change per drop while the sampling interval provided by hardware was around 3 ns at the sampling frequency used. Therefore, two or even three separate titrant drops would merge and be indistinguishable if the CoG was not used [18, Fig. 4]. The clusters of CoG related to the successive titrant additions border each other on the right side of Fig. 8, apparently due to the noise influence. Such clusters are not observable on the left-hand side of Fig. 8 because the time domain resolution, despite improvement achieved by using the CoG, was still limited.

VII. Application of the Temperature Correction to the Experimental Data for Experiments 2–5

In the case of experiment 1 (increasing concentration of electrolyte—$AlCl_3$) this correction did not lead to a notable difference in the recalculated ultrasonic titration curves, owing to a small change of temperature throughout the experiment ($+0.1$ °C). In contrast, correction for the temperature effect had a significant effect on the ultrasonic titration curve in the experiments 2 and 3 representing titrations of Al ions with strong and weak base, respectively [Fig. 7(a) and Fig. 9(a)]. The most profound change had occurred in the first part of the ultrasonic titration curves, before the maximum corresponding to the equilibrium point ($h = 3.0$, $t \sim 3600$ s for experiment 2 and $t \sim 1200$ s for experiment 3). This part was initially steadily decreasing, while after temperature correction it was increasing up to the maximum, which became the global maximum of the ultrasonic titration curve. Therefore, when the temperature effect was effectively removed from the ultrasonic data, the physically meaningful increase of ultrasonic delay corresponds mainly to the increase of "solid loading" of the Al-ion solution being titrated, as well as, in more general

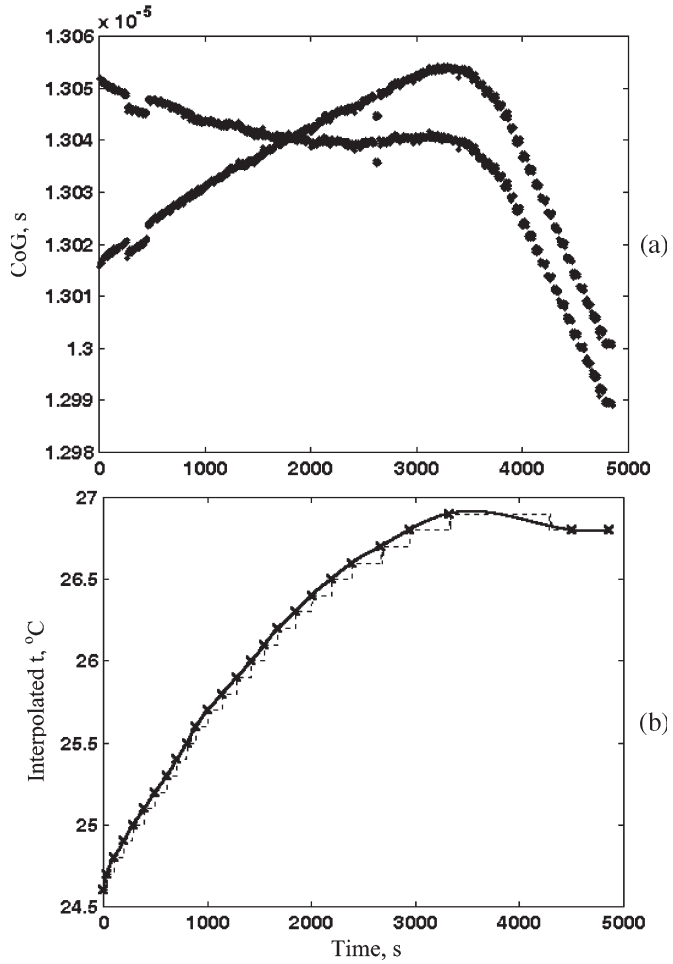

Fig. 7. Both (a) corrected and original propagation times and (b) spline interpolated temperature for experiment 2.

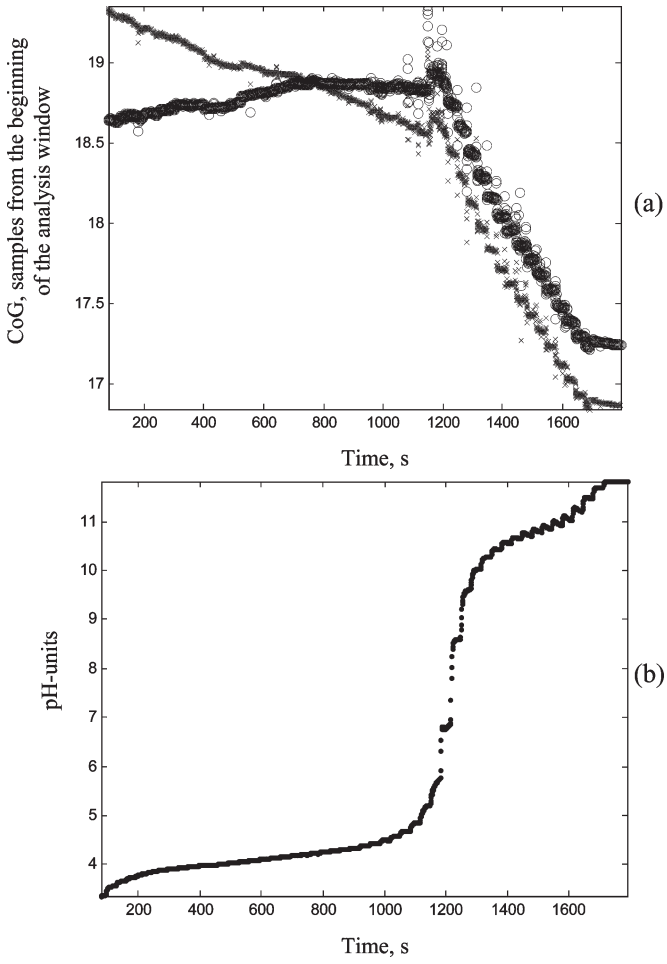

Fig. 9. Ultrasonic [(a) both original and compensated] and (b) pH titration curves for experiment 3.

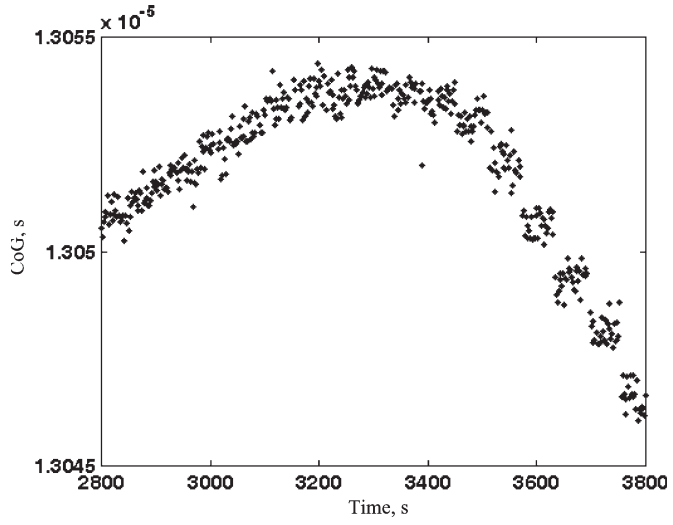

Fig. 8. Corrected propagation times around their maximum for the experiment 2.

terms, overall decrease of degrees of freedom of the condensing system in question.

A comparison of higher and lower concentration of a hard base (KOH or NaOH) in experiments 2 and 3 shows a steeper incline of the ultrasonic curve in the case of the higher base concentration. This is most probably related to the increasing "solid loading" in the system during the course of titration due to premature formation of colloidal Al hydroxide, which is less profound when a lower alkali concentration is used.

It is necessary to note that a slightly different experimental setup was used for experiment 3. Ultrasonic parameters were monitored by the same probe but with a different, custom designed data acquisition instrument. Also, in experiment 3, the pH and the ultrasonic measurements were synchronized much more precisely. In order to preserve compatibility of ultrasonic records, the sampling frequency to the transducer central frequency ratio was kept at the same value, providing 16 samples per period of the recorded waveform.

Both pH and ultrasonic curves of the titration experiment 3 (Fig. 9) are in good agreement with the results of experiment 2 [Figs. 4 and 7(a)]. The initial part of the ultrasonic curve shows some bias related to the rest of data. It happened due to an adjustment of the gain of the preamplifier during the experiment to avoid the ADC saturation. Theoretically the CoG estimate should eliminate the influence of the gain, but this observation shows that some noise remaining after averaging could cause bias. Therefore, the overall transfer coefficient of the instrument should be kept unchanged throughout the experiments. Both

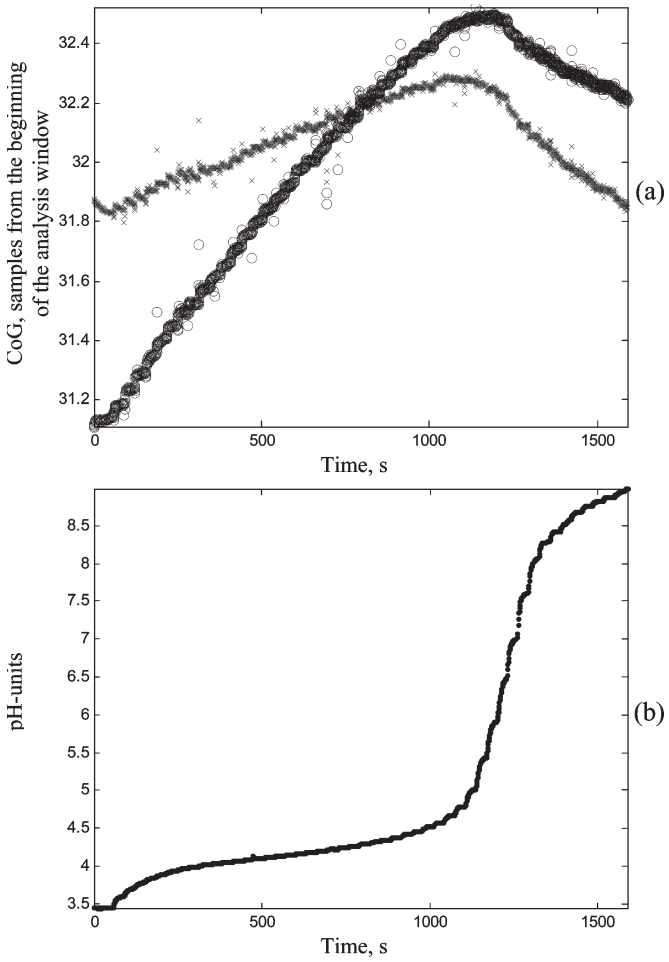

Fig. 10. Ultrasonic [(a) both original and compensated] and (b) pH titration curves for experiment 4.

curves show identical equivalence point at 1200 s by crossing the neutral level [pH = 7, pH curve, Fig. 9(a) and (b)]. After applying temperature compensation, the ultrasonic delay curve has a maximum at exactly the equivalence point [ultrasonic curve, Fig. 9(a)]. The latter curve could be more convenient for the purposes of process control when the reaction should continuously run at equilibrium [19]. This is because controlling the crossing of a particular level is prone to noise and calibration bias, while controlling the maximum is much more resilient to these factors.

A closer look at the ultrasonic curve reveals much smaller scatter in the ultrasound data than in the previous experiments (about 10 times) that was achieved due to averaging that became feasible with the use of the designed instrument. It was found that averaged data did not contain spikes in the resulting waveform observed previously. As the records were taken more frequently, it became possible to evaluate the time interval required to come to equilibrium after a transition (dropping chemical). In most cases that time was found close to 5 s that were required for stabilizing ultrasonic readings after the addition of alkali.

Experiments 4 and 5 involved softer bases—ammonium hydroxide and sodium sulphate (Table II). Fig. 10 presents

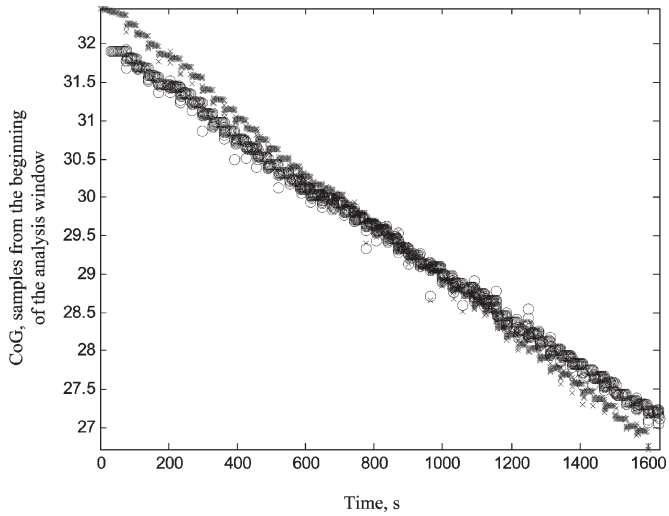

Fig. 11. Original and compensated ultrasonic titration curves for experiment 5.

the titration curves for experiment 4, where pH curves are compliant with the weak acid-weak base titration curve [14], and the ultrasound delay curve is very similar to the previously discussed experiments with hard bases (KOH and NaOH) and shows a distinct maximum. The equivalence point of both curves matches the calculated value at $h = 3.0$. The temperature-corrected ultrasonic curve differs from the previous ultrasonic curves by the higher value of the gradient in the rising slope and relatively steadier slope of the decreasing part of the curve. Significant gradient of the slope before the inflexion point at $h = 3.0$ despite the lower strength of alkali used (NH_4OH) can be explained in terms of well-known structure-breaking salvation behavior of ammonium-ion. This particular ion tends to disturb the structure of "liquid-crystalline" water formed by multiple hydrogen bonds, and this effect can lower elasticity of aqueous medium. This could also be a reason for the fact that additions of ammonia to Al-ions create significant amounts of flaky amorphous Al hydroxide at quite acidic pH (significantly lower than pH = 7.0).

The observed steadiness of the decreasing slope above equivalence point at $h = 3.0$ $(t = 1200$ s$)$ in the ultrasonic delay curve [Fig. 10(a)] could be explained by relative weakness of ammonia as a base $(\text{pKa} = 9.6)$ and its inability to dissolve amorphous Al hydroxide formed as a result of neutralization of Al-ions.

The softest base (sodium sulphate) was used for the titration of Al ions in experiment 5. In this experiment, both pH-metric and ultrasonic titration curves did not show any inflexions (Fig. 11 for the ultrasonic data). The temperature variation detected with the external thermo sensor was quite small. Therefore, there was no significant interaction between sulphate-ions and Al ions, which correlates well with the thermodynamic data. Overall, pH data changed very little in experiment 5 within 0.14 units pH, while the ultrasonic curve showed both the permanent trend and easily distinguishable states (Fig. 11) after each titrant addition and was similar to the curve obtained in the experiment 1 (Fig. 2).

VIII. Conclusion

Averaging and the use of CoG were found to be essential signal processing procedures for process monitoring of the hydrolysis observed and for obtaining more informative ultrasonic titration curves. The developed data acquisition instrument allowed an increase in the number of data points and the fidelity of the acquired records compared to the commercially available instrument that resulted in much less scatter of the ultrasonic titration curve.

An important distinction of this paper is the application of temperature compensation for ultrasonic curves using the reference data for pure solvent (here—water) rather than thermostating the reacting solution to eliminate its influence. This allows for *in situ* measurements in conventional reaction vessels using a dipstick probe. The temperature compensation allowed separation of contributions caused by temperature changes from contributions of other factors affecting elasticity of the medium (viscosity, ionic strength, structure-forming properties of solutes; in the case of heterogeneous systems—surface/interfacial tension; particle size; particle hydration) that were of primary interest.

Ultrasonic spectroscopy offers a much higher resolution in the time domain and a faster detection of chemical changes than pH-metry. The use of time-resolved ultrasonic titrations also allows to measure the mixture stabilization time after each titrant addition. This is very difficult for pH-metric measurement due to quite a significant time lag.

The ability of ultrasonic velocity measurements to detect precisely the equivalence point in the neutralization of Al chloride with base has been demonstrated in the present investigation. This allows for potential replacement of commonly used pH-metry with ultrasonic spectroscopy as a very robust and fast *in situ* method for fast monitoring of similar processes.

The increasing slope of the temperature-corrected ultrasonic titration curve mainly indicates increase of the "solid content" or "solid loading" in the system due to formation of Al hydroxide. The nearly linear shape of this part of the ultrasonic titration curve appears to be a result of continuous Al hydroxide formation even at relatively low pH where it is caused by local pH gradients rather than the actual chemical equilibrium. As a consequence, the slope of the increasing part of the ultrasonic titration curve is the highest for the hardest bases used (KOH and NaOH). For ammonium hydroxide it is also high, although this time it is caused by the structure-breaking properties of ammonium-ion involved in the titration. In the case of a very weak base (sodium sulphate), there was no detectable interaction with Al-ions, and therefore, the ultrasonic curve was nearly as linear as for the experiment with electrolyte solution ($AlCl_3$ in HCl).

The decreasing part of the ultrasonic titration curve occurs mainly due to 1) release of free hydroxyl ions and 2) dissolution of Al hydroxide formed at the equivalence point at $h = 3.0$ (maximum in the ultrasonic titration curve and the major jump on the pH-metric curve). It was observed that the stronger the base, the steeper the slope of the decaying part of the ultrasonic titration curve was.

A single ultrasonic measurement for a custom built instrument was completed in less than 0.5 s (this time included averaging of 1024 separate records). On this basis, the time required to reach equilibrium after a drop of the chemical was estimated at about 5 s.

References

[1] D. A. Skoog, D. M. West, and F. J. Holler, *Fundamentals of Analytical Chemistry*. Orlando, FL: Harcourt, 1996.

[2] R. E. Challis, M. J. Powey, M. L. Mather, and A. K. Holmes, "Ultrasound techniques for characterizing colloidal dispersions," *Rep. Progr. Phys.*, vol. 68, no. 7, pp. 1541–1637, Jul. 2005.

[3] F. Priego-Capote and M. D. Luque de Castro, "Analytical uses of ultrasound I: Sample preparation," *Trends Anal. Chem.*, vol. 23, no. 9, pp. 644–653, 2004.

[4] Z. Galbács, H. Van Langenhove, and G. Galbács, "The effect of sonification on glass electrodes," *Talanta*, vol. 66, pp. 809–812, 2005.

[5] J. Stuehr and E. Yeager, "The propagation of ultrasonic waves in electrolytic solutions," in *Physical Acoustics: Principles and Methods*, vol. II, pt. A. New York: Academic, 1965, pp. 351–462.

[6] J. P. M. Trusler, *Physical Acoustics and Metrology of Fluids*. Bristol, PA: IOP, 1991.

[7] J. Lamb, "Thermal relaxation in liquids," in *Physical Acoustics: Principles and Methods*, vol. II, pt. A, New York: Academic, 1965, pp. 203–281.

[8] T. A. Litovitz and C. M. Davis, "Structural and shear relaxation in liquids," in *Physical Acoustics: Principles and Methods*, vol. II, pt. A. New York: Academic, 1965, pp. 282–350.

[9] P. Resa, L. Elvira, F. Montero de Espinosa, and Y. Gomez-Ullate, "Ultrasonic velocity in water–ethanol–sucrose mixtures during alcoholic fermentation," *Ultrasonics*, vol. 43, no. 4, pp. 247–252, 2005.

[10] F. Priego-Capote and M. D. Luque de Castro, "Analytical uses of ultrasound II: Detectors and detection techniques," *Trends Anal. Chem.*, vol. 23, no. 10/11, pp. 829–838, 2004.

[11] R. C. Asher, *Ultrasonic Sensors*. Bristol, PA: IOP, 1997.

[12] C. C. Perry and K. L. Shafran, "The systematic study of aluminium speciation in medium concentrated aqueous solutions," *J. Inorg. Biochem.*, vol. 87, no. 1/2, pp. 115–124, Nov. 2001.

[13] K. L. Shafran, O. Deschaume, and C. C. Perry, "The static anion exchange method for generation of high purity aluminium polyoxocations and monodisperse aluminium hydroxide nanoparticles," *J. Mater. Chem.*, vol. 15, pp. 3415–3423, 2005.

[14] W. L. Masterton and C. N. Hurley, *Chemistry: Principles and Reactions*. Orlando, FL: Harcourt, 2001.

[15] A. J. Downs, Ed., *Chemistry of Aluminium, Gallium, Indium and Tallium*. London, U.K.: Chapman & Hall, 1993.

[16] C. Baird, *Environmental Chemistry*. New York: Freeman, 2003.

[17] A. N. Kalashnikov, K. L. Shafran, R. E. Challis *et al.*, "Super resolution *in situ* monitoring of chemical reactions," in *Proc. IEEE Ultrason. Symp.*, Montreal, QC, Canada, 2004, pp. 549–552.

[18] K. L. Shafran, C. C. Perry, V. Ivchenko, R. E. Challis, A. K. Holmes, and A. N. Kalashnikov, "Resolving complex chemical processes: Comparison of monitoring by ultrasound with other measurement methods," in *Proc. IEEE Instrum. Meas. Technol. Conf.*, Sorrento, Italy, 2006, pp. 714–719.

[19] H. Tominaga and M. Tomaki, Eds., *Chemical Reaction and Reactor Design*. Hoboken, NJ: Wiley, 1997.

[20] A. N. Kalashnikov and R. E. Challis, "Errors and uncertainties in the measurement of ultrasonic wave attenuation and phase velocity," *IEEE Trans. Ultrason., Ferroelectr., Freq. Control*, vol. 52, no. 10, pp. 1754–1768, Oct. 2005.

[21] *Ultrasonic Pulser Receiver*. (2006, Jun.). [Online]. Available: ndtsolutions.com.

[22] A. N. Kalashnikov, V. Ivchenko, and R. E. Challis, "VLSI architecture for repetitive waveform measurement with zero overhead averaging," in *Proc. IEEE Int. Symp. WISP*, Faro, Portugal, 2005, pp. 334–339.

[23] J. E. Bradshaw and N. E. Pedersen, "Acoustic flowmeter with envelope midpoint tracking," U.S. Patent 4 480 485, Nov. 6, 1984.

[24] R. E. Challis, T. Alper, A. K. Holmes, and R. P. Cocker, "Near-plane-wave acoustic propagation measurements in thin-layers of adhesive polymer," *Meas. Sci. Technol.*, vol. 2, no. 1, pp. 59–68, Jan. 1991.

[25] V. A. DelGrosso and C. W. Mader, "Speed of sound in pure water," *J. Acoust. Soc. Amer.*, vol. 52, no. 5B, pp. 1442–1446, Nov. 1972.

[26] A. N. Kalashnikov, V. Ivchenko, R. E. Challis, and A. K. Holmes, "Compensation for temperature variation in ultrasonic chemical process monitoring," in *Proc. IEEE Ultrason. Symp.*, Rotterdam, The Netherlands, 2005, pp. 1151–1154.

Alexander N. Kalashnikov (M'02) was born in Odessa, Ukraine, in 1962. He received the degree in electrical and acoustical engineering, the Candidate of Science (Ph.D.) degree by thesis on surface acoustic wave devices, and the Doctor of Science degree by thesis from Odessa State Polytechnic University (OSPU) in 1984, 1991, and 1999, respectively.

Between 1984 and 1999, he was with OSPU as an Engineer, Junior Researcher, Ph.D. Student, Lecturer, Senior Lecturer, Associate Professor, Doctorate, and Chief Researcher, and he published more than 80 articles, including four patents. He was a Research Associate with Loughborough University, Loughborough, U.K., in 1999. In 2001, He was with the School of Electrical and Electronic Engineering, University of Nottingham, Nottingham, U.K., as a Lecturer, and has published more than 20 articles since.

Dr. Kalashnikov is a member of the American Chemical Society (by invitation) and was awarded a Senior Researcher qualification by the Ukraine Supreme Qualification Committee in 1997.

Kirill L. Shafran was born in Ukraine in 1970. He received the Diploma degree in chemistry from Odessa State University (OSU), Odessa, Ukraine, in 1992 and the Ph.D. degree from Nottingham Trent University (NTU), Nottingham, U.K., in 2003.

From 1990 to 1996, he was with the Department of Analytical Chemistry, OSU, as a Laboratory Assistant, an Engineer, and then as a postgraduate student. In 1998, he defended the Ph.D. thesis on the adsorption of dyes and metal ions on silica for chemical sensing of trace metals. From 1996 to 1999, he was a Senior Scientific Researcher with the analytical group of the Department of Ecotoxicology, Ukrainian Research Institute of Medicine on Transport, Odessa. In 1999, he was with the inorganic and materials chemistry group of Prof. C. C. Perry at NTU, first, as a postgraduate student and then, from 2002 to 2005, as a Postdoctoral Researcher. In this research group, he became involved in structural and speciation studies of aqueous chemistry of aluminum and zirconium, as well as interactions of various inorganic species with biomolecules. In 2006, he was with Unilever Research and Development Centre, Port Sunlight, U.K., as a Research Scientist.

Vladimir G. Ivchenko received the degree and the Ph.D. degree in electrical engineering from Taganrog State University of Radioengineering (TSURE), Taganrog, Russia, in 1993 and 1997, respectively.

From 1993 to 2004, he was with TSURE as a Hardware Design/Verification Engineer, Research Assistant, and Assistant Professor. He was with the School of Electrical and Electronic Engineering, University of Nottingham, Nottingham, U.K., as a Research Fellow in 2004. His principal research interest is in the application-specific integrated circuit and field-programmable gate-array-based architectures for ultrasonics and nondestructive evaluation, applied optics, signal processing, and communications.

Richard E. Challis was born in the U.K. in 1945. He received the B.Sc. (Eng) and Ph.D. degrees in electrical engineering from the Imperial College of Science, Technology, and Medicine, London, U.K., in 1967 and 1975, respectively.

He has worked in the electrical engineering industry and in the health service in the U.K. He was Professor of engineering physics at the University of Keele, U.K., and subsequently Head of the School of Electrical and Electronic Engineering at the University of Nottingham, Nottingham, U.K. His principal area of research is instrumentation for industrial manufacturing and processes, with particular emphasis on quality assurance techniques for adhered metal assemblies and for colloidal materials in process.

He is a Fellow of the Institution of Electrical Engineers, a Fellow of the Institute of Physics, and a Fellow of the British Institute of Non-Destructive Testing. He was elected a Fellow of the Royal Academy of Engineering in 2004.

Carole C. Perry is a Professor of bioinorganic and materials chemistry and Head of Chemistry, Nottingham Trent University, Nottingham, U.K. Her research interests include fundamental studies of *in vivo* and *in vitro* silicon-biomolecule interactions (proteins, including collagen and carbohydrates). Her other main research area involves the preparation and characterization of aqueous and nonaqueous sol-gel derived materials.